Molecular motions of adsorbed CO2 on a tetrazole-functionalized PIM polymer studied with 13C NMR

Moore, Jeremy K.; Guiver, Michael D.; Du, Naiying; Hayes, Sophia E.; Conradi, Mark S.

Publisher's version / Version de l'éditeur:
https://doi.org/10.1021/jp4084234
The Journal of Physical Chemistry C, 117, 44, pp. 22995-22999, 2013-10-15

THE JOURNAL OF PHYSICAL CHEMISTRY C

Article

pubs.acs.org/JPCC

Molecular Motions of Adsorbed CO_2 on a Tetrazole-Functionalized PIM Polymer Studied with ^{13}C NMR

Jeremy K. Moore,[†] Michael D. Guiver,[§] Naiying Du,[§] Sophia E. Hayes,[†] and Mark S. Conradi*[,†,‡]

[†]Department of Chemistry, Washington University, One Brookings Drive, Saint Louis, Missouri 63130, United States

[‡]Department of Physics, Washington University, One Brookings Drive, Saint Louis, Missouri 63130, United States

[§]National Research Council Canada, Ottawa, Ontario K1A OR6, Canada

ABSTRACT: The CO_2 adsorption in a polymer of intrinsic microporosity (PIM) functionalized by tetrazole (TZPIM) has been studied with in situ ^{13}C nuclear magnetic resonance (NMR) spectroscopy at variable temperature and loading conditions. The CO_2 molecules are seen to interact with tetrazole sites through physisorption. The adsorbed system was studied from 8 to 385 K at two loadings of CO_2. The ^{13}C NMR resonance lineshapes and relaxation times have been analyzed to give insights into the adsorption process. The CO_2 molecules undergo site to site hopping with accompanying CO_2 reorientations while adsorbed on TZPIM, resulting in line narrowing starting near 100 K. Correspondingly, the spin echo T_2 passes through a minimum at 100 K. The analysis indicates that two kinds of adsorption sites are available.

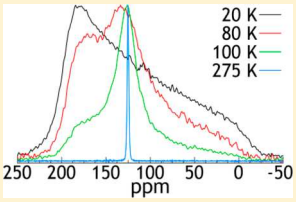

INTRODUCTION

Membrane-based technologies have many important applications in industrial processes such as microfiltration, ultrafiltration, reverse osmosis, electrodialysis, and gas separations as well as medicinal applications.[1] A very important potential application is postcombustion CO_2 capture from power plants and other large point sources of CO_2 emission.[2,3] The emissions from these point sources typically consist of approximately 15% CO_2 and 80% N_2. Current technologies for CO_2 separation from a mixed gas stream have many drawbacks, which include a large energy penalty for regeneration of the sorbent, low loading capacity, and physical degradation.[4] Therefore, improvements in CO_2 capture materials can make this technology viable for carbon capture, utilization, and storage applications being envisioned for reducing atmospheric CO_2 worldwide.[3]

Membrane-based capture is a potentially energy efficient technology for CO_2 separation.[5−10] Membrane materials must be engineered to allow selective gas permeation, such that the membranes serve as molecular-level filters, allowing the preferential passage of CO_2. Polymers of intrinsic microporosity (PIMs)[11,12] are promising membrane materials for CO_2 capture because they exhibit ultrahigh CO_2 permeability, suitable for the enormous volumes of CO_2 emitted from flue gas stacks. Tetrazole functionalized PIMs (TZPIM)[5] and their methyl derivatives[13] have demonstrated both high CO_2 permeability and good CO_2/N_2 selectivity for mixed gas separation.

Utilizing variable temperature in situ nuclear magnetic resonance (NMR) spectroscopy at multiple loadings of $^{13}CO_2$, the adsorption of CO_2 capture materials can be studied by examining the ^{13}C resonances from the CO_2 gas and adsorbed species within the material. The distinctive characteristics of the adsorption interactions can be determined with NMR. This study examines the molecular level dynamics of CO_2 adsorbed on TZPIM; it adds to the previous macroscopic studies on permeability, selectivity, and adsorption isotherms to better understand the adsorption properties of this material.[5] Combined, the macroscopic and NMR results provide an insight into the mode of CO_2 sorption, which will assist in the optimization of the sorbents and therefore aid the search for CO_2 separation technologies for environmental sustainability.

EXPERIMENTAL SECTION

The material studied here is a tetrazole functionalized polymer of intrinsic microporosity (TZPIM), synthesized by [2 + 3] cycloaddition postpolymerization reaction as described previously.[5] The polymer forms micropores that allow for high gas permeability due to the combination of a rigid backbone and sites of contortion in the polymer that frustrate efficient chain packing. The polymer contains two tetrazole groups per repeat unit, and it is these groups that interact favorably with CO_2. Although the tetrazole groups are located uniformly in every repeat unit of the polymer chain, they are randomly oriented in the polymer, as opposed to metal−organic frameworks (MOFs), which have one-dimensional channels.[14−16]

Each NMR experiment was started by packing approximately 100 mg of TZPIM powder into a glass tube followed by a bake out procedure. The bake out was at 80 °C under vacuum for 24 h to degas the sample of any adsorbed gases. A known quantity of ^{13}C-enriched CO_2 was introduced to each sample through a gas manifold. The tubes were cooled to 77 K so that the CO_2 was fully condensed, and 0.9 atm of He gas was introduced for thermal contact at low temperatures, then the tube was flame-sealed.

Received: August 22, 2013
Revised: October 11, 2013
Published: October 15, 2013

   dx.doi.org/10.1021/jp4084234 | J. Phys. Chem. C 2013, 117, 22995−22999

Variable temperature ^{13}C NMR studies below 200 K were performed in a Kadel helium research dewar coupled to a home-built NMR probe at a ^{13}C resonance frequency of 50.819 MHz in a 4.7 T magnet. Studies acquired above 200 K were performed on a laboratory-built NMR probe coupled to a stream of evaporated liquid nitrogen or heated air. Data were acquired with typical $\pi/2$ pulse lengths of 6 μs and 6 s recycle delays, averaging 64 transients. Samples were made at two CO_2 loadings, 0.12 and 0.33 mmol, and the samples contained 110 mg (sample 1) and 102 mg (sample 2) of TZPIM, respectively. These amounts give loadings (x) of 0.30 and 0.88 CO_2 molecules per tetrazole unit. These loadings were confirmed from the isotherm for CO_2 adsorption on TZPIM reported previously.[5]

RESULTS AND DISCUSSION

Figure 1 depicts a comparison of spectra collected both with and without the presence of TZPIM to confirm the type of interaction between CO_2 and the polymer. Both measurements were conducted with a 1 atm pressure of $^{13}CO_2$ gas at room temperature. The spectrum without the polymer is asymmetric due to the nonuniformity of the static magnetic field. For the equivalent overpressure of $^{13}CO_2$, the sample with the polymer shows no chemical shift change, an increase in line width, an increase by a factor of 9.3 in the ^{13}C signal integrated intensity, and an increase in T_1, the spin–lattice relaxation time, from 43.5 to 419 ms. These observations are expected for physisorption of CO_2 by the TZPIM. The CO_2 molecules have the same electronic cloud when constrained by the weak van der Waals interactions that drive physisorption, so the chemical shift is nearly unchanged. The increase in line width occurs because of magnetic field distortion by the small magnetic susceptibility of TZPIM. The increase in signal intensity shows that more CO_2 is present in the physisorbed sample, as compared to the gas-only sample, for the same 1 atm of gaseous CO_2 present. Clearly, most of the CO_2 is adsorbed under the conditions of Figure 1. The increase in T_1 reflects the much faster intrinsic relaxation in the gas phase.

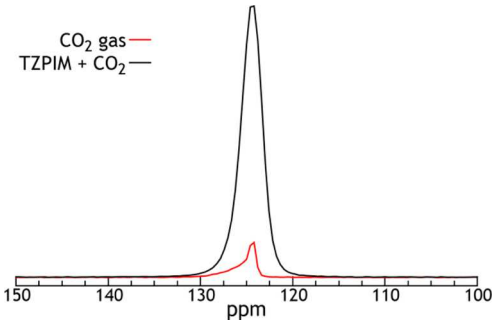

Figure 1. ^{13}C NMR resonances of CO_2 adsorbed on TZPIM as compared to CO_2 gas. Both are at a pressure of 1 atm and at 295 K.

To further investigate the adsorption of CO_2 on TZPIM, variable temperature ^{13}C NMR studies were performed on the CO_2-loaded polymer between 8 and 385 K. CO_2 was added such that, over the temperature range, approximately a constant amount of CO_2 was adsorbed on the polymer. That is, the sealed sample container has minimal gas-phase volume, so that nearly all the loaded CO_2 is adsorbed and a nearly constant sample loading is achieved.

Sample 1 was loaded with an amount of $^{13}CO_2$ gas corresponding to 0.30 CO_2 molecules per tetrazole unit. This loading was chosen because it is in the regime where every CO_2 molecule can access a tetrazole group on the polymer. By comparison, sample 2 was loaded with 0.88 CO_2 molecules per tetrazole unit. Here, each CO_2 molecule may not find a tetrazole group because the pore space is crowded. Some tetrazole units will be sterically hindered and inaccessible to CO_2 molecules. The CO_2 molecules in sample 1 can each find an accessible tetrazole adsorption site. In sample 2, each accessible tetrazole group will have a CO_2 molecule associated with it, while the extra CO_2 molecules will bind to less favorable adsorption sites.

In Figure 2, the ^{13}C NMR resonances depicted are for the temperatures given in the legends. These spectra were taken from echoes with a short pulse spacing of 50 μs. The ^{13}C NMR line shapes are seen to narrow over the range of temperatures studied, from 8 to 385 K. The low loading sample has a lower signal-to-noise ratio simply because there are fewer ^{13}C nuclei present in the sample.

Three line broadening interactions are present in these samples with CO_2 sorbed onto the polymer surface: chemical shift anisotropy (CSA),[17] characteristic of the linear CO_2; $^{13}C—^{1}H$ dipolar coupling between the sorbed $^{13}CO_2$ and hydrogen in the TZPIM polymer walls; and $^{13}C—^{13}C$ homonuclear dipolar coupling between $^{13}CO_2$ molecules. The CSA appears to be the dominant line broadening (see 40 K spectra), as expected.

At and below 80 K, in both the low and high loading samples, an axially symmetric powder pattern appears that exhibits the characteristic CSA of solid CO_2,[18,19] indicating sorbed CO_2 molecules with nearly fixed orientations on the NMR time scale (10^{-4} seconds). Each tetrazole unit on the polymer has a fixed orientation with respect to the external magnetic field. Because of the random nature of the polymer, the overall orientation distribution of the tetrazole groups is isotropic. This leads to an isotropic distribution of static CO_2 molecular orientations, giving rise to the CSA powder pattern line shape. The 40 K spectra are best described by $\Delta\sigma$ = 290 ppm, close to the values found in solid CO_2 (325 ppm)[18] and in another adsorbed system (315.3 ppm).[15,16] As the temperature increases in this regime (up to 80 K), the line shape narrows slightly due to the partial orientational averaging of the CSA, as will be discussed later.

At higher temperatures, reorientations of the CO_2 molecules result from site-to-site translational hopping because each adsorption site has a different orientation. Therefore, a molecular reorientation will occur simultaneously with each translational hop. Since the adsorption sites are at different orientations to the external magnetic field, the result is motional averaging of the CSA interaction, with line narrowing evident starting at 80 K (high loading) or 100 K (low loading) in Figure 2. We note that similar combined translation-reorientation events are found in solid CO_2,[18] α-CO,[20] N_2O,[21] and benzene[22] and also in CO_2 adsorbed onto a MOF.[15,16]

The translational hopping between the randomly oriented binding sites and resulting reorientations of the CO_2 molecules at higher temperatures lead to a single, symmetric ^{13}C resonance at a chemical shift of 125 ppm (that is, the CSA is time-averaged to zero). This line can be fit to a Lorentzian line shape, which narrows as the temperature is increased from 125 K. This signifies that the CO_2 molecules are more mobile (so hopping and reorienting more rapidly) at higher temperatures

dx.doi.org/10.1021/jp4084234 | J. Phys. Chem. C 2013, 117, 22995–22999

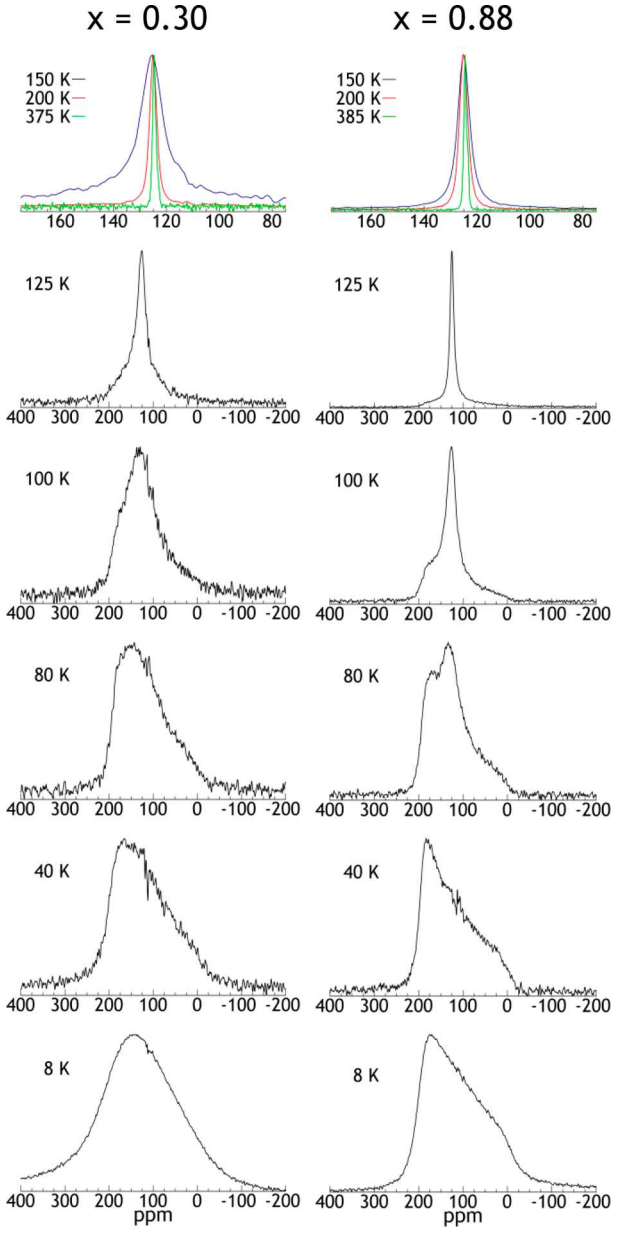

Figure 2. ^{13}C NMR resonances of CO_2 adsorbed on TZPIM. The spectra on the left are from the low loading sample, and the spectra on the right are from the high loading sample. The top spectra have an expanded *x*-axis to show the narrow resonances at higher temperatures; 100 ppm = 5.08 kHz.

as the van der Waals interactions between the sorbed gas and the TZPIM structure become less important relative to the thermal energy, k_BT. In the bulk solids CO_2, α-CO, and N_2O, the crystal symmetries are high enough (cubic) that the CSA is similarly time-averaged to zero by the combined translational and rotational motions. However, in the CO_2 adsorbed on Mg-MOF-74, the CO_2 molecules are confined to long hexagonal channels. There, even if the CO_2 molecules access, in the NMR time scale, all the binding sites on the channel, the CSA is averaged in general to a nonzero value. Thus, the $^{13}CO_2$ spectra in the MOF become axially symmetric powder patterns of reduced width in the fast averaging regime.[15,16]

According to Figure 2, in the low loading sample, the narrowing occurs in a single temperature step starting near 100 K. In the high loading sample, sample 2, the narrowing begins near 80 K. There, a subset of CO_2 molecules begins to hop at a lower temperature, which contributes to sample 2 narrowing at the lower temperature. The subset that hops more slowly is evident by the powder pattern that persists together with the narrowed feature. These two subsets are presumed to be on different adsorption sites, with the subset that keeps the powder pattern CSA line shape being more tightly bound. Since the low loading sample appears to narrow approximately at one temperature, the CO_2 molecules all have similar adsorption sites in this case.

Librational motions ("orientational rocking" in the bottom of the adsorption potential well) give rise to the small narrowing[23] that occurs up to 80 K. As mentioned above, as the temperature is increased, the molecules oscillate torsionally leading to a narrow distribution of θ values. θ is the angle between the CO_2 axis and the symmetry axis of the adsorption binding site. This distribution slightly decreases the time-average CSA and slightly narrows the resulting powder pattern. The oscillation can be thought of as the linear CO_2 molecule rocking about the binding axis with one oxygen molecule bound to the tetrazole unit. The width, $\Delta\sigma_{eff}$, of the powder pattern is determined by the following equation[24] when the CSA dominates the broadening:

$$\Delta\sigma_{eff} = \Delta\sigma\left(\frac{3}{2}\overline{\cos^2\theta} - \frac{1}{2}\right)$$

The term $\Delta\sigma$ is the width of the full CSA broadening for orientationally static CO_2. At the lowest temperatures, the CO_2 molecules sit at approximately $\theta = 0$. It should be noted that a head-to-tail flip of the CO_2 (flipping which oxygen is next to the tetrazole) will have no effect on the CSA because a head to tail flip adds π to the angle θ, leaving the cosine-squared term unaffected. The distribution of θ values grows larger as the temperature is increased, decreasing $\overline{\cos^2\theta}$ and decreasing slightly the width $\Delta\sigma_{eff}$.

The ^{13}C line width in Hz, found by the full width at half max of the NMR resonances, is plotted versus temperature in Figure 3. The line width is inversely proportional to the time constant T_2^*, which is the time for the NMR FID signal to decay. At low temperatures, when the CSA powder pattern line shape is apparent, the line width is nearly constant. Here, the small amount of narrowing is due to the torsional libration motions.

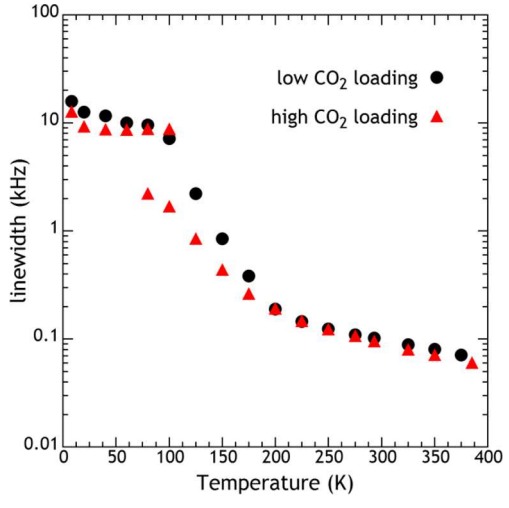

Figure 3. ^{13}C NMR line widths of CO_2 adsorbed on TZPIM.

dx.doi.org/10.1021/jp4084234 | J. Phys. Chem. C 2013, 117, 22995−22999

Above 100 K, the CO_2 molecules reorient faster due to the onset of translational hopping, so the ^{13}C line width decreases rapidly. When the CO_2 adsorbs in two types of sites, giving rise to two signals, both linewidths are plotted. The high loading sample has a smaller line width between 80 and 175 K due to the CO_2 molecules that are more weakly adsorbed. It is also seen that the onset of narrowing the line shape appears at a lower temperature for the high loading sample than the low loading sample.

The ^{13}C transverse relaxation time T_2 is determined from spin echoes and is plotted versus temperature in Figure 4. The

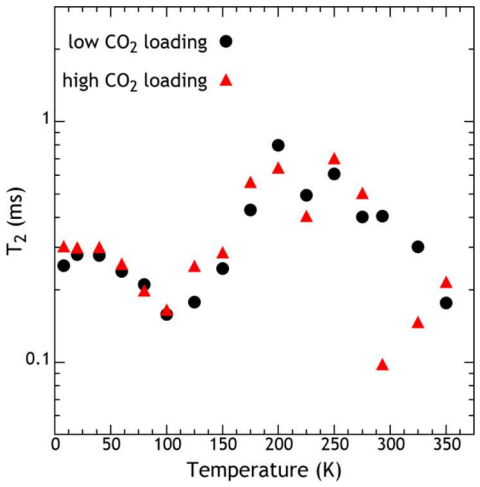

Figure 4. ^{13}C NMR T_2 relaxation time constant for CO_2 adsorbed on TZPIM.

relaxation time helps to differentiate the mechanisms of line narrowing.[18,25] At low temperatures, in the absence of reorientations, T_2 is determined by a combination of the $^{13}C—^{13}C$ dipolar coupling between $^{13}CO_2$ molecules and $^{13}C—^{1}H$ dipolar coupling between a $^{13}CO_2$ molecule and hydrogen from the TZPIM polymer chain. We note that the $^{13}C—^{13}C$ coupling is not time reversed by the ^{13}C π radio frequency pulse and the $^{13}C—^{1}H$ interaction is not refocused because of $^{1}H—^{1}H$ flip-flops driven by the $^{1}H—^{1}H$ dipolar couplings. Thus, both of these interactions contribute to echo attenuation. Both of these interactions are temperature independent at low temperatures where all hopping motion is frozen out, as evidenced by the T_2 plateau from 8 to 40 K. The data indicate that the $^{13}C—^{1}H$ coupling dominates because both the high and low loading samples share the same plateau value of T_2.

The decrease of T_2, from 40 to 100 K, is due to the onset of reorientational motion.[18,20] In this strong collision regime[20,26] of the relaxation time T_2, one hop of a given molecule causes the ^{13}C frequency to change sufficiently that this spin is well-dephased at the time of the spin echo. Therefore, in this regime the T_2 is approximately the mean time between hopping events. Every hop results in a reorientation, but the hops do not happen frequently enough for the $^{13}CO_2$ resonance to be motionally narrowed. The T_2 minimum occurs near the onset of line narrowing,[18] where the reorientations occur approximately once per the time-duration of the rigid-lattice FID (~100 μs). The minimum in the high loading sample is not as deep because there are two sites that narrow at different temperatures, as seen in the line shape. Above the T_2 minimum, T_2 and T_2* (as seen in the line width data) increase together due to the rapid hopping and reorienting of CO_2 molecules.

Above 150 K, T_2 has become longer than its low-temperature plateau value. That plateau value is determined by the dipolar interactions between $^{13}CO_2$ molecules and the ^{13}C interaction with the polymer protons. Thus, above 150 K both interactions are being averaged; this confirms that translational diffusion (site-to-site hopping) is rapid in this temperature range. The T_2 is not well understood at the highest temperatures, above 250 K; a fraction of CO_2 may be exchanging between the adsorbed and gas phase, which could lead to the observed T_2 behavior.

At very low temperatures, such as at 8 K, the CSA powder pattern line shapes show an additional broadening of the spectral features, as seen in Figure 2. The effect is particularly evident for the lower loading sample. We note that the spin–echo T_2 in Figure 4 shows no change at the lowest temperatures, demonstrating that the additional line broadening is refocused by the ^{13}C π radio frequency pulse, so it is an inhomogeneous broadening. All molecular motion is already frozen out at and below 80 K, so molecular motions are not involved in this additional broadening. We propose that the broadening is due to electronic magnetic moments and their contribution to the material's magnetic susceptibility. For free spins, this contribution will decrease as $1/T$ at high temperature, following Curie's Law. We note that the electron spin energy splitting at 4.7 T is about 132 GHz, or 6.6 K in temperature units. So the electronic spin polarization should be large (nearly 40%) at 8 K. Thus, electronic spins would cause a line broadening at low temperature and less broadening at higher temperatures. We note similar broadening in earlier work on CO_2 adsorbed on a MOF.[15,16]

The NMR spin–lattice relaxation time, T_1, is plotted versus temperature in Figure 5.[27] Samples 1 and 2 are offset in T_1 yet

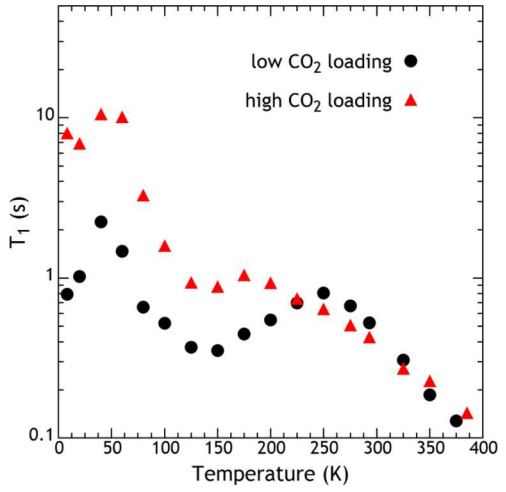

Figure 5. ^{13}C NMR T_1 relaxation time constant for CO_2 adsorbed on TZPIM.

follow the same trends. The T_1 decreases from 40 to 125 K, which corresponds to the onset of site-to-site hopping of the CO_2 molecules. Here, localized relaxation by isolated paramagnetic impurities may be spatially distributed by the increasingly rapid CO_2 diffusion.

The T_1 decreases for sample 1 above 250 K and for sample 2 above 175 K. These decreases are due to exchange of CO_2 between the gas and adsorbed phases. A complete model for this exchanging system is complicated and requires knowledge

dx.doi.org/10.1021/jp4084234 | J. Phys. Chem. C 2013, 117, 22995–22999

of the intrinsic gas-phase[28] and adsorbed-phase relaxation rates as well as the rate of exchange of CO_2 between the two phases. However, the following facts are relevant. First, the T_1 of $^{13}CO_2$ gas at 1 atm and 300 K is about 0.06 s, a much faster relaxation rate than for the adsorbed molecules (see Figure 5). Thus, a small amount of CO_2 in the gas phase could account for the increasingly rapid relaxation observed above 250 K. Second, the exchange rate between adsorbed and gas phases will naturally increase as the equilibrium CO_2 gas pressure increases. Thus, the exchange model broadly describes the high-temperature T_1 data of Figure 5.

The low loading sample starts its T_1 decrease at a higher temperature (250 K) because all the CO_2 molecules are bound to the best adsorption sites, on top of the tetrazoles. The subset of molecules in the high loading sample that are adsorbed on the less favorable sites result in a higher gas pressure at a given temperature, so the decrease in T_1 due to gas-adsorbed exchange occurs at a lower temperature.

CONCLUSIONS

The dynamics of CO_2 molecules adsorbed on TZPIM have been studied with in situ variable temperature ^{13}C NMR at two loadings of $^{13}CO_2$. It is seen that the adsorbed molecules are able to hop from site to site while adsorbed on the polymer. The hopping motion begins with infrequent jumps around 50 K, first evident as a decreasing spin−echo T_2. Once the temperature is raised above 100 K, the CO_2 molecules are able to rapidly hop from site to site. The reorientations that accompany the site-to-site translations time-average the primary source of line width, the CSA, and narrow the resonance. When the loading of CO_2 approaches 1 CO_2 per tetrazole unit, a second adsorption site becomes apparent. CO_2 on these second sites is less tightly bound, as demonstrated by the onset of line narrowing at a somewhat lower temperature. Understanding the dynamics of materials with applications in carbon capture will aid in the development of technologies that will allow for CO_2 storage and utilization.

AUTHOR INFORMATION

Corresponding Author

*(M.S.C.) Phone: 314-935-7334. E-mail: msc@wuphys.wustl.edu.

Notes

The authors declare no competing financial interest.

ACKNOWLEDGMENTS

We are grateful for funding through Washington University Consortium for Clean Coal Utilization. M.S.C. is grateful for DOE Basic Energy Sciences funding through grant DE-FG02-ER46256.

REFERENCES

(1) Baker, R. W. *Membrane Technology and Applications*; Wiley: New York, 2012.

(2) Jones, C. W. CO_2 Capture From Dilute Gases as a Component of Modern Global Carbon Management. *Annu. Rev. Chem. Biomol. Eng.* **2011**, *2*, 31−52.

(3) Samanta, A.; Zhao, A.; Shimizu, G. K. H.; Sarkar, P.; Gupta, R. Post-Combustion CO_2 Capture Using Solid Sorbents: A Review. *Ind. Eng. Chem. Res.* **2012**, *51*, 1438−1463.

(4) Bhown, A. S.; Freeman, B. C. Analysis and Status of Post-Combustion Carbon Dioxide Capture Technologies. *Environ. Sci. Technol.* **2011**, *45*, 8624−8632.

(5) Du, N.; Park, H. B.; Robertson, G. P.; Dal-Cin, M. M.; Visser, T.; Scoles, L.; Guiver, M. D. Polymer Nanosieve Membranes for CO_2-Capture Applications. *Nat. Mater.* **2011**, *10*, 372−375.

(6) Guiver, M. D.; Lee, Y. M. Polymer Rigidity Improves Microporous Membranes. *Science* **2013**, *339*, 284−285.

(7) Du, N.; Park, B.; Dal-Cin, M. M.; Guiver, M. D. Advances in High Permeability Polymeric Membrane Materials for CO_2. *Energy Environ. Sci.* **2012**, *5*, 7306−7322.

(8) Lin, H.; Freeman, B. D. Materials Selection Guidelines for Membranes That Remove CO_2 From Gas Mixtures. *J. Mol. Struct.* **2005**, *739*, 57−74.

(9) Merkel, T. C.; Lin, H.; Wei, X.; Baker, R. Power Plant Post-Combustion Carbon Dioxide Capture: An Opportunity for Membranes. *J. Membr. Sci.* **2010**, *359*, 126−139.

(10) Shao, P.; Dal-Cin, M. M.; Guiver, M. D.; Kumar, A. Simulation of Membrane-Based CO_2 Capture in a Coal-Fired Power Plant. *J. Membr. Sci.* **2013**, *427*, 451−459.

(11) Budd, P. M.; Elabas, E. S.; Ghanem, B. S.; Makhseed, S.; McKeown, N. B.; Msayib, K. J.; Tattershall, C. E.; Wang, D. Organophilic Membrane Derived From a Polymer of Intrinsic Microporosity. *Adv. Mater.* **2004**, *16*, 456−459.

(12) Budd, P. M.; Ghanem, B. S.; Makhseed, S.; McKeown, N. B.; Msayib, K. J.; Tattershall, C. E. Polymers of Intrinsic Microporosity (PIMs): Robust, Solution-Processable, Organic Nanoporous Materials. *Chem. Commun.* **2004**, 230−231.

(13) Du, N.; Robertson, G. P.; Dal-Cin, M. M.; Scoles, L.; Guiver, M. D. Polymers of Intrinsic Microporosity (PIMs) Substituted With Methyl Tetrazole. *Polymer* **2012**, *53*, 4367−4372.

(14) Queen, W. L.; Brown, C. M.; Britt, D. K.; Zajdel, P.; Hudson, M. R.; Yaghi, O. M. Site-Specific CO_2 Adsorption and Zero Thermal Expansion in an Anisotropic Pore Network. *J. Phys. Chem. C* **2011**, *115*, 24915−24919.

(15) Kong, X.; Scott, E.; Ding, W.; Mason, J. A.; Long, J. R.; Reimer, J. A. CO_2 Dynamics in a Metal−Organic Framework With Open Metal Sites. *J. Am. Chem. Soc.* **2012**, *134*, 14341−4.

(16) Lin, L. C.; Kim, J.; Kong, X.; Scott, E.; McDonald, T. M.; Long, J. R.; Reimer, J. A.; Smit, B. Understanding CO_2 Dynamics in Metal-Organic Frameworks With Open Metal Sites. *Angew. Commun.* **2013**, *52*, 4410−4413.

(17) Fukushima, E.; Roeder, S. B. W. *Experimental Pulse NMR: A Nuts and Bolts Approach*; Addison-Wesley Publishing Company: Boston, MA, 1981.

(18) Liu, S. B.; Doverspike, M. A.; Conradi, M. S. Combined Translation-Rotation Jumps in Solid Carbon Dioxide. *J. Chem. Phys.* **1984**, *81*, 6064−6068.

(19) Ratcliffe, C. I.; Ripmeester, J. A. ^1H and ^{13}C NMR Studies on Carbon Dioxide Hydrate. *J. Phys. Chem.* **1986**, *90*, 1259−1263.

(20) Liu, S.; Conradi, M. S. Combined Translational-Rotational Jumps in Solid Alpha-CO. *Phys. Rev. B* **1984**, *30*, 24−31.

(21) Ouyang, B.; Conradi, M. S. Nuclear-Magnetic-Resonance Determination of the Mechanism of Molecular Reorientation in Solid N_2O. *Phys. Rev. B* **1991**, *44*, 9295−9300.

(22) Gullion, T.; Conradi, M. S. Anisotropic Diffusion in Benzene: ^{13}C NMR Study. *Phys. Rev. B* **1985**, *32*, 7076−7082.

(23) Bayer, H. Theory of Spin−Lattice Relaxation in Molecular Crystals. *Z. Phys.* **1951**, *130*, 227.

(24) Mehring, M. *Principles of High Resolution NMR in Solids*, 2nd ed.; Springer: New York, 1983.

(25) Rothwell, W. P.; Waugh, J. S. Transverse Relaxation of Dipolar Coupled Spin Systems Under RF Irradiation: Detecting Motions in Solids. *J. Chem. Phys.* **1981**, *74*, 2721−2732.

(26) Slichter, C. P. *Principles of Magnetic Resonance*, 3rd ed.; Springer: New York, 1990.

(27) Etesse, P.; Zega, J. A.; Kobayashi, R. High Pressure Nuclear Magnetic Resonance Measurement of Spin−Lattice Relaxation and Selfdiffusion in Carbon Dioxide. *J. Chem. Phys.* **1992**, *97*, 2022−2029.

(28) Abragam, A. *The Principles of Nuclear Magnetism*; Oxford University Press: Oxford, U.K., 1973.